Biometals (2022) 35:173–185
https://doi.org/10.1007/s10534-021-00358-1

Synthesis and characterisation of phenanthroline-oxazine ligands and their Ag(I), Mn(II) and Cu(II) complexes and their evaluation as antibacterial agents

Muhib Ahmed · Sinead Ward · Malachy McCann · Kevin Kavanagh · Frances Heaney · Michael Devereux · Brendan Twamley · Denise Rooney

Received: 8 September 2021 / Accepted: 3 December 2021 / Published online: 17 January 2022

Abstract A series of phenanthroline-oxazine ligands were formed by a cyclisation reaction between L-tyrosine amino acid esters and 1,10-phenanthroline-5,6-dione (phendione). The methyl derivative of the phenanthroline-oxazine ligand **1** was complexed with Ag(I), Mn(II) and Cu(II) to form $[Ag(\mathbf{1})_2]ClO_4$, $[Mn(\mathbf{1})_3](ClO_4)_2$ and $[Cu(\mathbf{1})_3](ClO_4)_2$. The activity of these metal complexes was tested against the bacteria *Escherichia coli* and *Staphylococcus aureus*. Each of the metal complexes was more active than **1** against *S. aureus* and the Mn(II) and Cu(II) complexes also showed greater activity than **1** towards *E. coli*. The effect of increasing the length of the alkyl moiety on the phenanthroline-oxazine ligands and their corresponding *tris* homoleptic Cu(II) complexes was investigated. In all cases both the ligands and their complexes were more active against Gram-positive *S. aureus* than against Gram-negative *E. coli*. Differences in the lipophilicity of the ligands and their corresponding Cu(II) complexes did alter the antibacterial activity, with the hexyl and octyl derivatives and their complexes showing the greatest activity and comparing well with clinically used antibiotics. The most active Cu(II) complexes and their respective ligands were also active against Methicillin-resistant *S. aureus* (MRSA). In vivo toxicity studies, conducted using the *Galleria mellonella* model, showed that all of the compounds were well tolerated by the insect larvae.

Keywords Antimicrobial resistance · Phenanthroline · Metal complexes · Lipophilicity · Antibacterial activity · Oxazine

Supplementary Information The online version contains supplementary material available at https://doi.org/10.1007/s10534-021-00358-1.

M. Ahmed · S. Ward · M. McCann · F. Heaney · D. Rooney (✉)
Department of Chemistry, Maynooth University, Maynooth, Co. Kildare, Ireland
e-mail: denise.rooney@mu.ie

M. Ahmed · S. Ward · K. Kavanagh · F. Heaney · D. Rooney
Kathleen Lonsdale Institute for Human Health Research, Maynooth University, Maynooth, Co. Kildare, Ireland

K. Kavanagh
Department of Biology, Maynooth University, Maynooth, Co. Kildare, Ireland

M. Devereux
The Centre for Biomimetic & Therapeutic Research, Focas Research Institute, Technological University Dublin, City Campus, Camden Row, Dublin 8, Ireland

B. Twamley
School of Chemistry, Trinity College Dublin, The University of Dublin, Dublin 2, Ireland

Introduction

Bacterial antibiotic resistance is an ever increasing global threat to human health (Centers for Disease Control and Prevention 2013, 2014; World Health Organization 2014). Significantly, the World Health Organization (WHO) 2014 report, in which data from 129 member states were compiled, emphasised the large number of incidences of infections by resistant strains of bacteria in every region of the world, and the possible emergence of a 'post-antibiotic' era. Gram-positive *Staphylococcus aureus,* particularly the methicillin-resistant (MRSA) form, has been highlighted by WHO as one of nine bacterial species which are of international concern (World Health Organization 2014). MRSA is a major pathogen in both hospital and community-acquired infections and it can induce a number of superficial and systemic diseases (DeLeo and Chambers 2009; Malachowa and DeLeo 2010; Morell and Balkin 2010; Payne 2008; Schito 2006), and it is estimated that there are approximately 9000 MRSA related deaths in the US each year (Centers for Disease Control and Prevention 2014).

There is clearly an urgent need to develop the next generation of anti-bacterial therapeutics with different modes of action and as such, there is a growing interest in the medicinal applications of transition metal complexes (Graf and Lippard 2012; Hambley 2007; Ronconi and Sadler 2007). Metal complexes can adopt a range of coordination geometries and redox states allowing for greater chemical variation than is possible for organic molecules. As the complexes can carry a positive charge they may be attracted to negatively charged biological macromolecules such as oligonucleotides, and the binding affinity of metal complexes to DNA and RNA has been well studied (Łęczkowska and Vilar 2012). A number of metal complexes having good antimicrobial efficacy are currently in clinical use (Guo and Sadler 1999). For example, silver(I) sulfadiazine, which is commercially available as Silvadene, is used as a topical treatment for burn wounds (Mjos and Orvig 2014). Previous studies by our group have shown that Mn(II) phenanthroline-isoniazid complexes have good activity against a number of bacteria including *M. tuberculosis* (Ahmed et al. 2019b). There is much interest in the biological activity of copper complexes and there have been many recent reports on their antimicrobial and antiviral properties (Ali et al. 2021; Joseph et al. 2013; Liu et al. 2013). Copper ions are involved in the disruption of metalloproteins (Haeili et al. 2014), the generation of reactive oxygen species (Salah et al. 2021) the disruption of membrane integrity (Karlsson et al. 2013) and as a carrier of charged antibiotic compounds (Manning et al. 2014). Macrophages use copper as a form of a 'brass dagger' to expose microbes to excess copper as a defence mechanism (German et al. 2013). Excess copper can lead to a reduction of the pathogenic potential of bacteria. For example, the virulence factors of *S. aureus* are reduced and the ability to form a biofilm is significantly curtailed due to copper stress (Baker et al. 2010). Although copper is an essential metal required for the cell cycle, it has to be carefully regulated due to its inherent toxicity. Bacteria can sequester copper ions, use enzymes for detoxification and employ efflux mechanisms for the homeostasis of copper found inside and outside the cell (Bondarczuk and Piotrowska-Seget 2013). Consequently, copper complexes are of interest as a delivery method to allow for the passage of the metal ion through the bacterial cell envelope and to possibly target internal organelles and the DNA.

1,10-Phenathroline (phen) has garnered much interest in the field of cell biology as its rigid planar structure makes it a suitable DNA intercalator, while the two juxtaposed nitrogen atoms on the fused aromatic rings allow it to chelate metal ions. Phen and its metal complexes show a wide variety of biological activity, such as anti-tumour (Roy et al. 2008), anti-bacterial (Butler et al. 1969), anti-viral (Shulman and White 1973) and anti-fungal behaviour (Coyle et al. 2004). Numerous researchers have functionalised phen in order to enhance its effectiveness in different applications (Abel et al. 2020; Alreja and Kaur 2016; Luman and Castellano 2004). One of the most well-known and useful derivatives is 1,10-phenanthroline-5,6-dione (phendione). Metal complexes of phendione display a wide variety of biological activity which include anti-tumour (Kellett et al. 2012) and anti-bacterial activity (Viganor et al. 2016). Previously, our group synthesised the phenanthroline-oxazine ligand **1** by a Schiff base condensation reaction of phendione with the methyl ester of L-tyrosine (Scheme 1). The Ag(I) and Cu(II) *bis* complexes of **1** showed stronger binding to calf-thymus DNA than their phen analogues and also the minor groove binding drugs, pentamidine and netropsin (McCann et al. 2013). Herein, we report a further

expansion of this ligand family by making the Ag(I) *bis* complex (McCann et al. 2013), Mn(II) and Cu(II) *tris* complexes of **1** and also by lengthening the alkyl chain moiety of the L-tyrosine ester so as to alter the lipophilicity of the phenanthroline-oxazine ligands **2–5** and hence that of the corresponding Cu(II) *tris* complexes **7–10** (Table 1). The compounds were screened for their antibacterial activity against Gram-negative *Escherichia coli* and Gram-positive *S. aureus*, including MRSA. In addition, the in vivo toxicities of the compounds were established using the *Galleria mellonella* model.

Table 1 Metal Complexes formed using the phenanthroline-oxazine ligands

	Complex
6a[a]	$[Ag(\mathbf{1})_2]ClO_4$
6b	$[Mn(\mathbf{1})_3](ClO_4)_2$
6c	$[Cu(\mathbf{1})_3](ClO_4)_2$
7	$[Cu(\mathbf{2})_3](ClO_4)_2$
8	$[Cu(\mathbf{3})_3](ClO_4)_2$
9	$[Cu(\mathbf{4})_3](ClO_4)_2$
10	$[Cu(\mathbf{5})_3](ClO_4)_2$

[a]McCann et al. (2013)

Materials and methods

All chemicals were reagent grade and used without further purification, unless stated otherwise. Phendione was synthesised by a literature procedure (Zheng et al. 2010). Caution: extreme care must be exercised when handling perchlorate salts. Nutrient broth and Phosphate Buffered Saline (PBS) were obtained from Sigma Aldrich and prepared according to the manufacturer's instructions. The NMR spectra were recorded on a Bruker Avance spectrometer operating at 500 MHz for the ^{1}H nucleus and 126 MHz for the ^{13}C nucleus. The probe temperature was maintained at 25 °C. Residual solvent peaks were used as internal standard. FTIR spectra were recorded as KBr discs on a Perkin Elmer Spectrum 100 FT-IR spectrometer or a Nicolet iS50 FT-IR instrument. High Resolution Mass Spectrometry (HRMS) analysis was carried out on a ESI Agilent-L 1200 Series coupled to a 6210 Agilent Time-of-Flight (TOF) equipped with both a positive and negative electrospray source or a time-of-flight (MicrOTOF) mass spectrometer (Bruker Daltonik GmbH, Bremen, Germany), which was coupled to an Agilent HPLC stack (Agilent, Santa Clara, CA, United States) consisting of Agilent G1312A binary pump with G1329A autosampler and G1316A column oven. The CHN elemental analysis was carried out on a FLASH EA 1112 Series Elemental Analyser with Eager 300 operating software. Magnetic moment measurements were carried out on a Johnson Matthey Magnetic Susceptibility Balance with $Hg[Co(SCN)_4]$ used as the standard. The HPLC chromatograms were extracted from LC–MS studies that were performed on an Agilent Technologies 1200 Series instrument consisting of a G1322A Quaternary pump and a G1314B UV detector (254 nm) coupled to an Advion Expression L Compact Mass spectrometer (ESI) operating in positive mode. Separations were performed on a Waters Xbridge OST 2.5 µm, 4.6 × 50 mm column (C18) operating at a flow rate of 0.2 mL min^{-1}.

Scheme 1 Reaction of phendione with L-tyrosine ester hydrochlorides to form phenanthroline-oxazines **(1)–(5)**

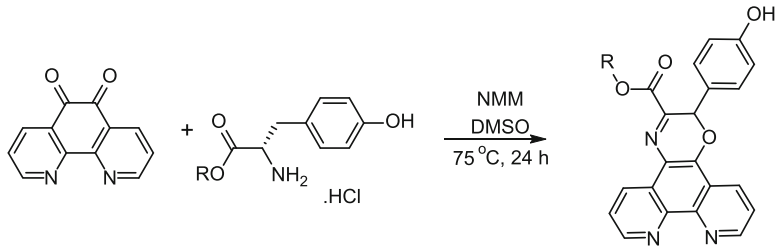

Ligand	1	2	3	4	5
R	Methyl	Propyl	Hexyl	Octyl	Dodecyl
Yield (%)	42	41	38	35	31

General synthesis of the L-tyrosine ester hydrochloride salts

This was carried out by appropriate modifications of reported ester syntheses (Buckley et al. 2010; Capilato et al. 2017). Acetyl chloride (4.35 mL, 50.3 mmol) was added to a cold solution of the appropriate alcohol (50 mL). To this, L-tyrosine (2.00 g, 11.0 mmol) was added and the resulting clear colourless solution was heated at reflux for 3 h. The resulting solution was filtered while hot and then the lower boiling alcohol solutions were reduced to 10 mL on a rotary evaporator. The product was precipitated via addition of 400 mL diethyl ether. The resulting white solid was filtered and washed with 3 × 50 mL portions of diethyl ether and dried under vacuum. The characterisation data of the hydrochloride salts were consistent with those reported in the literature; L-tyrosine methyl ester (Proteau-Gagné et al. 2010), L-tyrosine hexyl ester (Yang et al. 2011), L-tyrosine octyl ester (Joondan et al. 2014), and L-tyrosine dodecyl ester (Joondan et al. 2014).

General synthesis of the phenanthroline-oxazine ligands 1–5

L-Tyrosine ester hydrochloride salt (1 mmol) was dissolved in 25 mL of DMSO and to this solution, *N*-methylmorpholine (NMM) (0.121 mL, 1.12 mmol) was added. The solution was heated to 75 °C while being constantly stirred and phendione (0.210 g, 1.00 mmol) was then added to give a bright yellow solution. After constant stirring at 75 °C for 24 h, a clear bright orange solution was observed. After cooling to room temperature 125 mL of DCM was added. The organic layer was washed with 5 × 125 mL portions of H_2O and then dried over $MgSO_4$. The resulting DCM solution was condensed to dryness on a rotary evaporator to give the crude product. If a syrup was observed at this point, further washings with H_2O were required to remove traces of DMSO. The dried contents of the flask were dissolved in 15 mL of hot MeOH and the solution allowed to stand overnight. The resulting bright yellow crystalline solid was filtered, washed with 3 × 20 mL portions of MeOH and dried under vacuum.

Methyl 2-(4-hydroxyphenyl)-2H-[1,4]oxazino[2,3-f][1,10]phenanthroline-3-carboxylate (1)

The characterisation data were consistent with that given previously in the literature (McCann et al. 2013).

Propyl 2-(4-hydroxyphenyl)-2H-[1,4]oxazino[2,3-f][1,10]phenanthroline-3-carboxylate (2)

Yellow solid. **Yield:** 0.169 g, 41%. **mp:** decomp. @ 230 °C. **^{1}H NMR** (DMSO-d6, 500 MHz): **δ** 9.74 (br s, 1H, O**H**), 9.12 (dd, *J* = 4.3, 1.8 Hz, 1H, Phen**H**), 9.03 (dd, *J* = 4.3, 1.8 Hz, 1H, Phen**H**), 8.88 (dd, *J* = 8.3, 1.8 Hz, 1H, Phen**H**), 8.59 (dd, *J* = 8.3, 1.8 Hz, 1H, Phen**H**), 7.85 (dd, *J* = 8.3, 4.3 Hz, 1H, Phen**H**), 7.79 (dd, *J* = 8.3, 4.3 Hz, 1H, Phen**H**), 7.22–7.19 (m, 2H, Ar**H**), 6.69–6.66 (m, 2H, Ar**H**), 6.57 (s, 1H, oxazine-**H**), 4.30–4.21 (m, 2H, –OC**H$_2$**), 1.75–1.64 (m, 2H, C**H$_2$**), 0.91 (t, *J* = 7.5 Hz, 3H, C**H$_3$**). **^{13}C NMR** (DMSO-d6, 126 MHz): **δ** 162.6 (**C**=O), 159.2 (**C**–OH), 151.9 (Phen**C**), 150.6 (oxazine **C**=N), 149.1 (Phen**C**), 146.8 (Phen**C**), 142.7 (Phen**C**), 138.9 (Phen**C**), 131.4 (Phen**C**), 130.3 (Phen**C**), 129.4 (Ar**C**), 126.5 (Phen**C**-N), 125.5 (Ar**C**), 124.6 (Phen**C**), 124.2 (Phen**C**), 122.1 (Phen**C**), 121.7 (Phen**C**), 116.3 (Ar**C**), 72.7 (oxazine O**C**H), 67.7 (–O**C**H$_2$), 21.9 (**C**H$_2$), 10.6 (**C**H$_3$). **FTIR** (KBr, cm^{-1}): 3443, 2973, 1734, 1610, 1592, 1516, 1500, 1434, 1379, 1351, 1313, 1286, 1254, 1239, 1223, 1172, 1133, 1073, 1021, 969, 925, 831, 742, 678, 632. **HRMS** (ESI +): Calcd m/z for: $(C_{24}O_4N_3H_{19} + H)^+$ $[M + H]^+$ 414.1448, Found: 414.1440. **CHN (%)**: $C_{24}O_4N_3H_{19}.H_2O$ Calcd: C 66.81, H 4.91, N 9.74; Found: C 66.47, H 4.72, N 9.97.

Hexyl 2-(4-hydroxyphenyl)-2H-[1,4]oxazino[2,3-f][1,10]phenanthroline-3-carboxylate (3)

Yellow solid. **Yield:** 0.173 g, 38%. **mp**: 208–209 °C. **^{1}H NMR** (DMSO-d6, 500 MHz): **δ** 9.70 (s, 1H, O**H**), 9.12 (dd, *J* = 4.3, 1.8 Hz, 1H, Phen**H**), 9.03 (dd, *J* = 4.3, 1.8 Hz, 1H, Phen**H**), 8.88 (dd, *J* = 8.3, 1.8 Hz, 1H, Phen**H**), 8.58 (dd, *J* = 8.3, 1.8 Hz, 1H, Phen**H**), 7.84 (dd, *J* = 8.3, 4.3 Hz, 1H, Phen**H**), 7.78 (dd, *J* = 8.3, 4.3 Hz, 1H, Phen**H**), 7.21–7.17 (m, 2H, Ar**H**), 6.69–6.66 (m, 2H, Ar**H**), 6.57 (s, 1H, oxazine-**H**), 4.33–4.24 (m, 2H, -OC**H$_2$**), 1.69–1.63 (m, 2H, C**H$_2$**), 1.31–1.23 (m, 6H, 3 × C**H$_2$**), 0.86–0.83 (m,

3H, C**H**$_3$). **^{13}C NMR** (DMSO-d6, 126 MHz): **δ** 162.7 (**C**=O), 159.4 (**C**–OH), 152.1 (Phen**C**), 150.8 (oxazine **C**=N), 149.2 (Phen**C**), 147.0 (Phen**C**), 142.9 (Phen**C**), 139.0 (Phen**C**–O), 131.5 (Phen**C**), 130.4 (Phen**C**), 129.6 (Ar**C**), 126.7 (Phen**C**-N), 125.6 (Ar**C**), 124.7 (Phen**C**), 124.3 (Phen**C**), 122.3 (Phen**C**), 121.9 (Phen**C**), 116.4 (Ar**C**), 72.9 (oxazine O**C**H), 66.4 (–O**C**H$_2$), 31.4 (**C**H$_2$), 28.5 (**C**H$_2$), 25.6 (**C**H$_2$), 22.6 (**C**H$_2$), 14.5 (**C**H$_3$). **FTIR** (KBr, cm^{-1}): 3425, 2961, 1707, 1607, 1583, 1513, 1503, 1434, 1380, 1341, 1327, 1290, 1260, 1172, 1134, 1073, 1022, 956, 929, 840, 742, 684, 635. **HRMS** (ESI +): Calcd m/z for: $(C_{27}O_4N_3H_{25} + H)^+$ $[M + H]^+$ 456.1918, Found 456.1940. **CHN (%)**: $C_{27}O_4N_3H_{25}$ Calcd: C 71.19, H 5.53, N 9.22; Found: C 70.02, H 5.20, N 9.73.

Octyl 2-(4-hydroxyphenyl)-2H-[1,4]oxazino[2,3-f][1,10]phenanthroline-3-carboxylate (4)

Yellow solid. **Yield:** 0.169 g, 35%. **mp**: 213–215 °C. **^{1}H NMR** (DMSO-d6, 500 MHz): **δ** 9.70 (s, 1H, O**H**), 9.12 (dd, *J* = 4.3, 1.8 Hz, 1H, Phen**H**), 9.03 (dd, *J* = 4.3, 1.8 Hz, 1H, Phen**H**), 8.87 (dd, *J* = 8.3, 1.8 Hz, 1H, Phen**H**), 8.57 (dd, *J* = 8.3, 1.8 Hz, 1H, Phen**H**), 7.83 (dd, *J* = 8.3, 4.3 Hz, 1H, Phen**H**), 7.78 (dd, *J* = 8.3, 4.3 Hz, 1H, Phen**H**), 7.22–7.18 (m, 2H, Ar**H**), 6.69–6.65 (m, 2H, Ar**H**), 6.57 (s, 1H, oxazine-**H**), 4.34–4.24 (m, 2H, –OC**H$_2$**), 1.71–1.63 (m, 2H, C**H$_2$**), 1.33–1.20 (m, 10H, 5 × C**H$_2$**), 0.87–0.82 (m, 3H, C**H$_3$**). **^{13}C NMR** (DMSO-d6, 126 MHz): **δ** 162.5 (**C**=O), 159.3 (**C**–OH), 151.9 (Phen**C**), 150.6 (oxazine **C**=N), 149.1 (Phen**C**), 146.9 (Phen**C**), 142.7 (Phen**C**), 138.9 (Phen**C**-O), 131.4 (Phen**C**), 130.2 (Phen**C**), 129.4 (Ar**C**), 126.5 (Phen**C**-N), 125.4 (Ar**C**), 124.6 (Phen**C**), 124.2 (Phen**C**), 122.1 (Phen**C**), 121.7 (Phen**C**), 116.2 (Ar**C**), 72.7 (oxazine O**C**H), 66.2 (–O**C**H$_2$), 31.6 (**C**H$_2$), 29.04 (**C**H$_2$), 29.01 (**C**H$_2$), 28.4 (**C**H$_2$), 25.8 (**C**H$_2$), 22.5 (**C**H$_2$), 14.4 (**C**H$_3$). **FTIR** (KBr, cm^{-1}): 3435, 2925, 1739, 1609, 1594, 1578, 1517, 1501, 1432, 1375, 1314, 1277, 1238, 1173, 1137, 1071, 1022, 944, 930, 839, 818, 742, 676, 631. **HRMS** (ESI+): Calcd m/z for: $(C_{29}O_4N_3H_{29} + H)^+$ $[M + H]^+$ 484.2231, Found: 484.2240. **CHN (%)**: $C_{29}O_4N_3H_{29}$ Calcd: C 72.03, H 6.05, N 8.69; Found: C 71.67, H 6.29, N 9.14.

Dodecyl 2-(4-hydroxyphenyl)-2H-[1,4]oxazino[2,3-f][1,10]phenanthroline-3-carboxylate (5)

Yellow solid. **Yield:** 0.167 g, 31%. **mp**: 172–174 °C. **^{1}H NMR** (DMSO-d6, 500 MHz): **δ** 9.70 (s, 1H, O**H**), 9.11 (dd, *J* = 4.3, 1.8 Hz, 1H, Phen**H**), 9.02 (dd, *J* = 4.3, 1.8 Hz, 1H, Phen**H**), 8.87 (dd, *J* = 8.3, 1.8 Hz, 1H, Phen**H**), 8.56 (dd, *J* = 8.3, 1.8 Hz, 1H, Phen**H**), 7.82 (dd, *J* = 8.3, 4.3 Hz, 1H, Phen**H**), 7.76 (dd, *J* = 8.3, 4.3 Hz, 1H, Phen**H**), 7.21–7.18 (m, 2H, Ar**H**), 6.69–6.66 (m, 2H, Ar**H**), 6.56 (s, 1H, oxazine-**H**), 4.34–4.22 (m, 2H, -OC**H$_2$**), 1.68–1.62 (m, 2H, C**H$_2$**), 1.33–1.09 (m, 18H, 9 × C**H$_2$**), 0.78 (t, *J* = 6.9 Hz, 3H, C**H$_3$**). **^{13}C NMR** (DMSO-d6, 126 MHz): **δ** 162.5 (**C**=O), 159.3 (**C**–OH), 151.9 (Phen**C**), 150.5 (oxazine **C**=N), 149.0 (Phen**C**), 146.9 (Phen**C**), 142.8 (Phen**C**), 138.8 (Phen**C**-O), 131.3 (Phen**C**), 130.2 (Phen**C**), 129.4 (Ar**C**), 126.5 (Phen**C**-N), 125.4 (Ar**C**), 124.4 (Phen**C**), 124.1 (Phen**C**), 122.1 (Phen**C**), 121.7 (Phen**C**), 116.2 (Ar**C**), 72.7 (oxazine O**C**H), 66.2 (–O**C**H$_2$), 31.7 (**C**H$_2$), 29.5 (**C**H$_2$ × 2), 29.4 (**C**H$_2$ × 2)), 29.2 (**C**H$_2$), 29.0 (**C**H$_2$), 28.4 (**C**H$_2$), 25.8 (**C**H$_2$), 22.5 (**C**H$_2$), 14.3 (**C**H$_3$). **IR (KBr, cm^{-1}):** 3430, 2923, 1737, 1711, 1610, 1590, 1516, 1503, 1487, 1464, 1433, 1377, 1322, 1285, 1238, 1171, 1130, 1072, 1021, 956, 840, 810, 739, 677, 631. **HRMS** (ESI+): Calcd m/z for: $(C_{33}O_4N_3H_{37} + H)^+$ $[M + H]^+$ 540.2857, Found: 540.2857. **CHN (%)**: $C_{33}O_4N_3H_{37}$ Calcd: C 73.44, H 6.91, N 7.79; Found: C 72.38, H 7.80, N 8.16.

General Procedure for the synthesis of metal complexes of methyl 2-(4-hydroxyphenyl)-2*H*-[1,4]oxazino[2,3-*f*][1,10]phenanthroline-3-carboxylate 6a, b, c.

The metal complexes **6a-c** were synthesised by heating a solution/suspension of metal perchlorate salts and **1** at reflux in the appropriate metal salt:ligand molar ratios (Ag (I) (1:2 equiv, 0.13 mmol:0.260 mmol), Mn(II) (1:3 equiv, 0.174 mmol:0.519 mmol) and Cu(II)(1:3 equiv, 0.173 mmol:0.519 mmol) in methanol (40 mL) for 2 h. the resulting precipitates were filtered, washed with cold methanol and dried under vacuum.

[Ag(1)$_2$](ClO$_4$).2MeOH·H$_2$O (6a)

Yellow solid. **Yield**: 0.097 g, 70%. **^{1}H NMR** (DMSO-d6, 500 MHz): **δ** 9.75 (s, 2H, O**H**), 9.13 (dd, *J* = 4.5, 1.6 Hz, 2H, Phen**H**), 9.07–9.01 (m, 4H, Phen**H**), 8.77 (dd, *J* = 8.3, 1.6 Hz, 2H, Phen**H**), 8.04–7.93 (m, 4H, Phen**H**), 7.30–7.19 (m, 4H, Ar**H**), 6.71–6.68 (m, 4H, Ar**H**), 6.66 (s, 2H, oxazine-**H**), 3.93 (s, 6H, –OC**H$_3$**). **^{13}C NMR** (DMSO-d6, 126 MHz): **δ** 162.9 (**C**=O), 159.4 (Ar**C**), 153.0 (Phen**C**), 151.1 (oxazine **C**=N), 150.4 (Phen**C**), 143.3 (Phen**C**), 139.2 (Phen**C**), 139.2 (Phen**C**), 133.4 (Phen**C**), 132.4 (Phen**C**), 129.6 (Ar**C**), 127.2 (Phen**C**), 126.1 (Phen**C**), 125.8 (Phen**C**), 125.1 (Ar**C**), 122.4 (Phen**C**), 122.3 (Phen**C**), 116.3 (Ar**C**), 72.9 (oxazine O**C**H), 53.6 (–O**C**H$_3$). **FTIR** (KBr, cm^{-1}): 2953, 1714, 1611, 1509, 1435, 1346, 1260, 1173, 1101, 1032, 809, 734, 622. **HRMS** (ESI +): Calcd *m/z* for [Ag(C$_{22}$H$_{15}$N$_3$O$_4$)$_2$]$^+$: (M)$^+$ 877.1171; Found: (M)$^+$ 877.1198. **CHN (%)**: Calcd: [Ag(C$_{22}$H$_{15}$N$_3$O$_4$)$_2$](ClO$_4$).2MeOH·H$_2$O: C 52.11, H 3.80, N 7.93; Found: C 52.05, H 3.52, N 8.00.

[Mn(1)$_3$](ClO$_4$)$_2$·MeOH·2H$_2$O (6b)

Yellow solid. **Yield:** 0.134 g, 52%. **FTIR** (KBr, cm^{-1}): 2952, 1719, 1607, 1515, 1438, 1353, 1263, 1174, 1100, 1035, 813, 734, 623. **CHN (%)**: Calcd: [Mn(C$_{22}$H$_{15}$N$_3$O$_4$)$_3$](ClO$_4$)$_2$·MeOH·2H$_2$O: C 54.45, H 3.61, N 8.53; Found: C 54.51; H 3.61; N 8.52. **μ$_{eff}$** = 6.0 BM.

[Cu(1)$_3$](ClO$_4$)$_2$.2H$_2$O (6c)

Green solid. **Yield:** 0.072 g, 29%. **FTIR** (KBr, cm^{-1}): 2954, 1720, 1609, 1515, 1436, 1352, 1263, 1174, 1085, 1038, 813, 731, 624. **CHN (%):** Calcd: [Cu(C$_{22}$H$_{15}$N$_3$O$_4$)$_3$](ClO$_4$)$_2$·2H$_2$O: C 54.54, H 3.40, N 8.67; Found: C 54.30, H 3.62, N 8.41. **μ$_{eff}$** = 2.3 BM.

General procedure for the synthesis of the Cu(II) phenanthroline-oxazine complexes (7–10)

A 10 mL MeCN solution of Cu(ClO$_4$)$_2$·6H$_2$O (0.062 g, 0.17 mmol) was added to a stirring heated 40 mL MeCN suspension of ligands **2–5** (0.50 mmol). The resulting clear, luminescent green solution was heated at reflux for 2 h. The solution was reduced to 5 mL under vacuum. The product was precipitated via addition of *ca.* 400 mL diethyl ether, filtered, washed with 3 × 50 mL portions of diethyl ether, and dried under vacuum.

[Cu(2)$_3$](ClO$_4$)$_2$·2H$_2$O (7)

Green solid. **Yield:** 0.202 g, 80%. **FTIR** (KBr, cm^{-1}): 2966, 1713, 1610, 1515, 1438, 1353, 1265, 1174, 1086, 1037, 814, 732, 625. **CHN (%)**: Calcd: [Cu(C$_{24}$H$_{19}$N$_3$O$_4$)$_3$](ClO$_4$)$_2$·2H$_2$O: C 56.20, H 4.00, N 8.19; Found: C 56.36, H 3.79, N 8.18. **μ$_{eff}$** = 2.0 BM.

[Cu(3)$_3$](ClO$_4$)$_2$·2H$_2$O (8)

Green solid. **Yield:** 0.196 g, 81%. **FTIR** (KBr, cm^{-1}): 2954, 2928, 1714, 1610, 1515, 1452, 1438, 1352, 1260, 1174, 1101, 1037, 814, 732, 623. **CHN (%)**: Calcd: [Cu(C$_{27}$H$_{25}$N$_3$O$_4$)$_3$](ClO$_4$)$_2$·2H$_2$O: C 58.43, H 4.78, N 7.57; Found: C 57.72, H 4.71, N 7.79. **μ$_{eff}$** = 2.2 BM.

[Cu(4)$_3$](ClO$_4$)$_2$·CH$_3$CN (9)

Green solid. **Yield:** 0.176 g, 74%. **FTIR** (KBr, cm^{-1}): 2965, 2927, 1714, 1610, 1515, 1452, 1437, 1383, 1262, 1173, 1087, 1046, 814, 731, 626. **CHN (%)**: Calcd: [Cu(C$_{29}$H$_{29}$N$_3$O$_4$)$_3$](ClO$_4$)$_2$·CH$_3$CN: C 60.94, H 5.17, N 7.98; Found: C 60.78, H 5.11, N 8.20. **μ$_{eff}$** = 2.1 BM.

[Cu(5)$_3$](ClO$_4$)$_2$ (10)

Green solid. **Yield:** 0.180 g, 71%. **FTIR** (KBr, cm^{-1}): 2924, 2852, 1714, 1610, 1515, 1452, 1438, 1383, 1261, 1173, 1102, 1036, 813, 731, 622. **CHN (%)**: Calcd: [Cu(C$_{33}$H$_{37}$N$_3$O$_4$)$_3$](ClO$_4$)$_2$: C 63.20, H 5.95, N 6.70; Found: C 63.45, H 6.28, N 5.79. **μ$_{eff}$** = 2.1 BM.

Determination of bacterial cell minimum inhibitory concentrations

Cells (*S. aureus*, MRSA and *E. coli*) were cultured overnight in an aerated conical flask in an orbital shaker at 37 °C and 200 rpm in nutrient broth. The OD$_{600}$ of the bacterial culture was measured and the culture was diluted with nutrient broth to produce a bacterial suspension with OD$_{600}$ of 0.1. The stock

solutions of the compounds were prepared in two ways. (1) The stock solutions of the water-soluble parent metal salts were dissolved in neat DMSO to yield 4 mM stock solutions. The solutions were diluted to give a final concentration range tested against the microbial strains of 125–3.9 μM (all solutions contained nutrient broth ≤5% v/v DMSO). (2) The water-insoluble compounds (metal complexes and known antibacterial agents) were dissolved in neat DMSO and diluted with DMSO containing media to give final concentrations of the test compounds upon addition of bacterial suspension of 30–0.2344 μM (all solutions contained nutrient broth and 5% v/v DMSO). The bacterial suspension with OD_{600} of 0.1 was loaded (100 μL) into the 96 wells of the plate each well containing the solution of the test compounds (100 μL) to give the final concentration. The bacterial growth was measured at 600 nm after 24 h at 37 °C using a spectrophotometer (BioPhotometer).

In vivo toxicity testing towards *Galleria mellonella*

Compounds **1–5, 6a,b,c and 7–10** were dissolved in neat DMSO to produce 600 μM solutions. These were then diluted with neat DMSO to produce a series of solutions with concentrations in the range of 600–30 μM. Each solution was then diluted with deioinsed H_2O media (1:10 dilution) to yield stock solutions of concentration range of 60–3 μM. A control solution was also prepared using DMSO (10% v/v) in PBS. Sixth instar larvae were used for this testing. The larvae of the same age were weighed and the larvae with weight of 0.22–0.27 g were used. Five larvae were placed in a clean petri dish and injected with 20 μL solution of the appropriate compounds. The dose was administered through the last pro-leg of the insect using a Myjector U100 insulin syringe. The larvae were incubated for 24 h at 37 °C. The survival rate of the insect was monitored at 24, 48 and 72 h.

Lipophilicity determination of 1–5

The relative lipophilicity of the of the ligands **1–5** was examined via HPLC. Due to the solubility profile of these ligands, the conventional shake flask method (Andres et al. 2015) could not be utilised. Alternatively, the relative lipophilicity of **1–5** was calculated using the ChemDraw prime 16.1 programme to yield calculated octanol/water partition coefficient (*c* log *P*) values. Additionally, the retention times for **1–5** were obtained from high performance liquid chromatography (C18 column). Separations were performed using a mobile phase of 0.1% formic acid in water (Solvent A) and 0.1% formic acid in acetonitrile (Solvent B) and a linear gradient of 0–100% B over 30 min.

Results and discussion

Chemical synthesis

The phenanthroline-oxazine ligands (**1–5**) were synthesised by reacting phendione with the appropriate L-tyrosine ester hydrochloride (Scheme 1) and the compounds were isolated in moderate yield (31–42%). The first step of the reaction is a Schiff base condensation reaction between the amine group of the amino acid ester and one of the carbonyl moieties of phendione. Previous studies by our group have shown that the subsequent cyclisation reaction to form the phenanthroline-oxazine compound is favoured by having an electron-donating group (in this case hydroxyl) at the *para* position of the phenyl ring of the amino acid ester (Ahmed, et al. 2019a). X-ray crystal structures were obtained for compounds **2** (Figure S25), **3** (Figure S26), **4** (Figure S27) and **5** (Fig. 1 and S28). The ligands crystallise as a racemic mixture as is in keeping with a mechanism involving Schiff base formation, and a 1,5-prototropic isomerisation prior to cyclisation (Ahmed, et al. 2019a). The phenol rings in **2–5** are almost orthogonal to the oxazine ring, with angles of 82.2° for **5**, to 94.5° for **3**. A comparison of **2–5** with the few structurally known phenanthroline-oxazine derivatives show the expected overlay of the phenanthroline-oxazine moiety and the orientation of the aromatic substituents on the oxazine (Ahmed, et al. 2019a; McCann et al. 2013).

The metal complexes, **6a-c** were synthesised by heating a solution/suspension of metal perchlorate salts and ligand **1** in the following metal:ligand molar ratio: {Ag (I) (1:2), Mn(II) (1:3) and Cu(II) (1:3)} in methanol. The Cu(II) complexes (**7–10**) were prepared by heating an acetonitrile suspension of $Cu(ClO_4)_2.6$-H_2O with the appropriate ligand in a 1:3 molar ratio. The complexes were characterised by elemental

Fig. 1 Schematic molecular structure of rac-(*R,S*)-**5: A** The *S*-configuration of **5** and **B** The *R*-configuration of **5**. Aside from the hydrogen at the stereogenic carbon atom only heteroatoms are labelled for clarity

analysis, IR spectroscopy (Figures S13, 16–21) and magnetic susceptibility. Elemental analysis clearly supports the $Cu(L)_3$ structure. ^1H and ^{13}C NMR spectra were recorded for the diamagnetic Ag(I) complex **6a** (Figure S14 and S15). The IR spectra of complexes **7–10** shows frequency shifts in some of the ligand absorption bands that are characteristic of metal complexation. Bands associated with the phenanthroline aromatic ring stretching (at *ca.* 1610, 1585 and 1500 cm^{-1}) were shifted to slightly higher wavenumbers upon complexation. The band at *ca* 740 cm^{-1}, assigned to the out-of-plane bending vibration of the phenanthroline C-H bonds, shifts to lower wavenumber (ca. 734 cm^{-1}) as previously observed for other Cu(II) phenanthroline complexes. Bands at *ca.* 1100 and 622 cm^{-1} which are present in the IR spectra of the metal complexes are indicative of the presence of the uncoordinated perchlorate counterion (Campos-Vallette et al. 1996). The magnetic moments of the Cu(II) complexes **6c** and **7–10** were between 2.0 and 2.3 BM and are comparable with the value calculated using the spin-only formula (1.7 BM), while that for the Mn(II) complex **6b** was 6.0 BM close to the calculated value (5.9 BM).

Antimicrobial activity

One way to enhance the antibacterial effect of a therapeutic agent is to boost the uptake of the compound by the microbe and a possible means of achieving this is by increasing the lipophilicity of the agent. This is based on the Overton's concept that lipid-soluble compounds will pass more easily through the lipid membrane surrounding the bacterial cell and therefore lead to an increase in antimicrobial activity (Hannesschlaeger et al. 2019). Dwyer and co-workers were the first to demonstrate this relationship between lipophilicity and antibacterial activity for phenanthroline complexes when they showed that the antibacterial activity of $[Ru(phen)_3]^{2+}$ increased upon addition of methyl substituents to the phenanthroline ligand (Dwyer et al. 1969). More recently, in a report by Kumar et al. on ruthenium(II) tris-homoleptic complexes, modifications were made to the pyridyl-1,2,3-triazole based ligands via elongation of the alkyl chain (butyl, hexyl, octyl, dodecyl and hexadecyl) on the triazole moiety in order to alter the lipophilicity of the complexes. Although these Ru(II) complexes were inactive against Gram-negative *E. coli*, the length of the alkyl chain did influence the activity against Gram-positive *S. aureus*, with the hexyl and octyl derivatives being the most effective (Kumar et al. 2016).

In a similar way the lipophilicity of ligands **1–5** was altered by increasing the length of the alkyl chain of the ester group on the L-tyrosine moiety. The inhibitory effects of the metal-free ligands **1–5** on *S. aureus and E. coli*, along with their *c*-log *P* values and HPLC retention times, are given in Table 2. The range of concentrations of the compounds (0.23–30 μM) investigated was limited by their lack of solubility at concentrations > 30 μM in the growth medium, which also contained 5% v/v DMSO (DMSO itself had essentially no inhibitory effect on microbial growth at this concentration). Upon progressing from methyl to octyl, the level of antimicrobial activity against *S. aureus* increased with increasing lipophilicity of the ligand. Interestingly, this inverse relationship between the MIC value and the length of the alkyl chain did not extend to the most lipophilic derivative, the dodecyl ester compound (**5**). This compound was relatively inactive and had MIC values similar to those of the least lipophilic member of the family, the

Table 2 Growth inhibitory effects of ligands **1–5** *on S. aureus* and *E. coli* and their associated *c*-log *P* and retention times (determined using HPLC)

Compound	*S. aureus* MIC (μM)		*E. coli* MIC (μM)		*c*-log *P*	Retention Time* (min)
	MIC_{50}	MIC_{80}	MIC_{50}	MIC_{80}		
1	> 30	> 30	> 30	> 30	2.8	21.7
2	8	9	> 30	> 30	3.6	22.5
3	2	4	> 30	> 30	4.9	27.8
4	2	3	> 30	> 30	5.7	30.7
5	> 30	> 30	> 30	> 30	7.4	35.4

> 30 μM MIC_{50} and MIC_{80} were outside the range of concentrations of compounds studied (3.75–30 μM). n = 16

[a]HPLC retention times determined using a 2.5 μm, 4.6 × 50 mm column (C18); mobile phase 0.1% formic acid in water (A) to 0.1% formic acid in acetonitrile (B), linear gradient of 0–100% (B) over 30 min

methyl derivative (**1**). In contrast, all of the ligands were essentially inactive against Gram-negative *E. coli* over the range of concentrations studied. This decrease in activity is likely to due to the inability of the complexes to reach their intracellular targets, possibly due to a combination of active efflux and the ability of the outer membrane surrounding the Gram-negative bacterial cells to deter penetration by certain agents (Krishnamoorthy et al. 2017).

A range of metal complexes of the phenanthroline-oxazine ligands were also screened against *S. aureus* and *E. coli* (Table 3). Although the metal-free ligand **1** was essentially inactive against *S. aureus*, the *bis* Ag(I), and *tris* Mn(II) and Cu(II) complexes of **1** (**6a–c**) had good activity, with the Cu(II) complex being the most active. The Cu complex, **6c**, was also the most active against Gram-negative *E. coli,* displaying moderate MIC_{50} and MIC_{80} values. Significantly, in general, each of the metal complexes showed greater anti-bacterial activity than their respective parent perchlorate metal salt. This enhancement in the activity of the metal cation upon complexation has been commonly observed and can be explained by Tweedy's chelation theory (Memon et al. 2016; Pitchumani Violet Mary et al. 2019; Viganor et al. 2017). Upon chelation to a ligand, such as the phenanthroline-oxazine compounds described here, the polarity of metal ion is reduced due to overlap with the ligand orbitals and partial sharing of the positive charge of the metal ion with the N-donor atoms of the chelating phenanthroline moiety. In addition, there is π-electron delocalisation over the ligand which augments the overall lipophilicity of the complex.

As the Cu(II) complex **6c** had shown better activity than the Ag(I) complex **6a** and the Mn(II) complex **6b** a series of Cu(II) *tris*-complexes of the other

Table 3 Antimicrobial activities of test complexes, simple metal salts and known antibacterial agents against *S. aureus* and *E. coli*

Compound	*S. aureus* MIC (μM)		*E. coli* MIC (μM)		Compound	*S. aureus* MIC (μM)		*E. coli* MIC (μM)	
	MIC_{50}	MIC_{80}	MIC_{50}	MIC_{80}		MIC_{50}	MIC_{80}	MIC_{50}	MIC_{80}
6a	15	> 30	> 30	> 30	$AgClO_4$	72	> 125	83	125
6b	19	28	26	> 30	$Mn(ClO_4)_2{\cdot}6H_2O$	> 125	> 125	> 125	> 125
6c	9	12	24	28	$Cu(ClO_4)_2{\cdot}6H_2O$	> 125	> 125	> 125	> 125
7	4	4	22	28	Ampicillin	> 30	> 30	> 30	> 30
8	1	2	> 30	> 30	Doxycycline	9	> 30	5	> 30
9	1	2	> 30	> 30	Streptomycin	10	> 30	1	3
10	> 30	> 30	> 30	> 30	Tetracycline	6	> 30	> 30	> 30
					Vancomycin	2	3	20	> 30

phenanthroline-oxazine ligands (**2**–**5**) were synthesised. These were tested against the two bacteria to determine if the increase in lipophilicity of the complex also influenced its anti-bacterial activity in a similar manner to that of the ligands. The results for all the Cu(II) complexes (**6c**, **7**–**10**) are given in Table 3 and for comparison purposes, the MIC values of several clinically used antibiotics were also measured. As was generally found for the metal-free ligands, the activity of the *tris*-homoleptic Cu(II) complexes against *S. aureus* improved with increasing alkyl chain length of the ligand. Similar to the study by Kumar et al. of Ru(II) complexes of 2-(1-substituted–1*H*-1,2,3-triazol-4-yl)pyridine (Kumar et al. 2016), the best activity was achieved by the hexyl- and octyl-alkyl chain derivatives, with the present Cu(II) complexes, **8** and **9**, respectively, both having MIC_{50} = 1 μM and MIC_{80} = 2 μM. These two Cu(II) complexes were essentially twice as effective as the most active clinical antibiotic, vancomycin. Again, as was found for the docecyl derivative **5**, its corresponding Cu(II) complex (**10**) was ineffective below a concentration of 30 μM. Just as reported by Kumar et al., there appeared to be a 'sweet spot' in the relationship between lipophilicity and antibacterial activity. We are not presently commenting on whether the lipophilicity contribution is manifested chiefly at the complex uptake stage or if its impact is more keenly felt in other aspects of biological action. As recently reported the stability and speciation of metal complexes in the incubation media are important characteristics to be considered when probing the mechanism of biological activity (Nunes et al. 2020).

Interestingly, the activity of the Cu(II) complexes against *E. coli* did not follow a similar trend to that observed for *S. aureus*, with only the least lipophilic complexes **6c** and **7** showing activity in the range of concentrations studied with **6c** and **7** both showing marginal activity (MIC_{80} value of 28 μM).

The complexes are a mixture of isomers as the ligands are formed in a racemic mixture and in addition it is likely that the Cu(II) complexes (**6c**, **7**–**10**) form as *fac* and *mer* isomers. No attempt was made to separate the isomers, so at this stage we cannot determine if one isomer is more active than another.

Values of > 30 μM denote that MIC_{50} and MIC_{80} were outside the range of concentrations of compounds studied (3.75–30 μM). Values of > 125 μM denote that MIC_{50} and MIC_{80} were outside the range of concentrations of parent perchlorate metal salts studied (39–125 μM). n = 16.

As the metal-free ligands **3** and **4** and their respective Cu(II) complexes, **8** and **9**, were the most active of the test compounds these were then screened against MRSA (Table 4). Although the MIC_{50} value for **3** is similar against MRSA and *S. aureus*, the MIC_{80} value for MRSA has increased by a factor of 2.5. For ligand **4**, and the MIC_{50} and MIC_{80} values for MRSA have both increased by *ca.* fourfold compared to *S. aureus*. Whilst the Cu(II) complexes **8** and **9** showed similar activity to *S. aureus* and MRSA they were more active against MRSA than their respective metal-free ligands, **3** and **4: 8** and **9** showed comparable activity to vancomycin (Appleman and Citron 2010; Sancak et al. 2013).

In vivo toxicity studies of the ligands and complexes using the wax moth larvae *Galleria mellonella*

The insect *Galleria mellonella* (Greater wax moth) belongs to the order Lepidoptera and has been widely utilised in various biological screening studies of potential drug candidates (Cook and McArthur 2013). The immune system of this insect closely resembles the innate immune system of mammals (Dinh et al. 2021) and the *G. mellonella* model can provide a great deal of useful information about the pharmacokinetic and pharmacodynamics associated with an administered agent (Piatek et al. 2020).

Solutions of the ligands **1**–**5** and the metal complexes **6a,b,c**, **7**–**10** (30, 15 and 7.5 μM) in 10% v/v DMSO in PBS were each injected into a batch of 5 larvae and the responses monitored every 24 h over a total period of 72 h. Positive controls were set up using

Table 4 Activity of metal-free ligands **3** and **4** and their respective *tris*Cu(II) complexes, **8** and **9**, against MRSA

Compound	MRSA MIC (μM)	
	MIC_{50}	MIC_{80}
3	2	10
4	8	14
8	1	3
9	1	1

n = 16

a 10% v/v DMSO solution in PBS. In all cases a 100% survival was seen and there were no visible signs of melanisation, indicating that an immune response had been prompted. The larvae were then left at 37 °C for a further two weeks and all of them developed into adult moths, demonstrating that the injected compounds did not disrupt the *G. mellonella* life cycle. These results indicate that, at the concentrations studied, the test compounds were well tolerated in vivo by *G. mellonella* and are likely to be non-toxic to mammalian models.

Conclusions

Phenthanthroline-oxazine ligands of varying lipophilicity are readily prepared by reacting phendione with a range of L-tyrosine alkyl esters, and homoleptic transition metal complexes can subsequently be synthesised. Compared to the metal-free ligand **1** (methyl ester), the Ag(I), Mn(II) and Cu(II) complexes are more active against Gram-positive *S. aureus*, whilst the Mn(II) and Cu(II) complexes have greater activity against Gram-negative *E. coli*. The phenthanthroline-oxazine metal complexes also have better antibacterial effects than their parent simple metal perchlorate salts. A 'sweet spot' is evident in the lipophilicity/activity relationship of the Cu(II) complexes, **6c, 7–9**, against *S. aureus*, with the hexyl and octyl derivatives, **8** and **9**, showing the highest activity. The Cu(II) complexes, **8** and **9**, are also effective against MRSA. Importantly, all the ligands and their Cu(II) complexes are well tolerated in vivo by *G. mellonella* larvae.

Acknowledgements We gratefully acknowledge a Maynooth University John and Pat Hume Scholarship Award for MA and a MU Studentship for SW.

Funding Maynooth University, National University of Ireland,Maynooth

Declarations

Conflict of interest The authors have no conflicts of interest to declare that are relevant to the content of this article.

References

Abel AS, Averin AD, Beletskaya IP, Bessmertnykh-Lemeune A (2020) Transition-metal-catalyzed functionalization of 1,10-phenanthrolines and their complexes. Targets Heterocycl Syst 24:419–444. https://doi.org/10.17374/targets.2021.24.419

Ahmed M, Rooney D, McCann M, Casey J, O'Shea K, Twamley B (2019a) Tuning the reaction pathways of phenanthroline-Schiff bases: routes to novel phenanthroline ligands. Dalton Trans 48(40):15283–15289. https://doi.org/10.1039/c9dt03084k

Ahmed M, Rooney D, McCann M, Devereux M, Twamley B, Galdino ACM, Sangenito LS, Souza LOP, Lourenco MC, Gomes K, Dos Santos ALS (2019b) Synthesis and antimicrobial activity of a phenanthroline-isoniazid hybrid ligand and its Ag(+) and Mn(2+) complexes. Biometals 32(4):671–682. https://doi.org/10.1007/s10534-019-00204-5

Ali A, Sepay N, Afzal M, Sepay N, Alarifi A, Shahid M, Ahmad M (2021) Molecular designing, crystal structure determination and in silico screening of copper(II) complexes bearing 8-hydroxyquinoline derivatives as anti-COVID-19. Bioorg Chem 110:104772. https://doi.org/10.1016/j.bioorg.2021.104772

Alreja P, Kaur N (2016) Recent advances in 1,10-phenanthroline ligands for chemosensing of cations and anions. RSC Adv 6(28):23169–23217. https://doi.org/10.1039/c6ra00150e

Andres A, Roses M, Rafols C, Bosch E, Espinosa S, Segarra V, Huerta JM (2015) Setup and validation of shake-flask procedures for the determination of partition coefficients (logD) from low drug amounts. Eur J Pharm Sci 76:181–191. https://doi.org/10.1016/j.ejps.2015.05.008

Appleman MD, Citron DM (2010) Efficacy of vancomycin and daptomycin against *Staphylococcus aureus* isolates collected over 29 years. Diagn Microbiol Infect Dis 66(4):441–444. https://doi.org/10.1016/j.diagmicrobio.2009.11.008

Baker J, Sitthisak S, Sengupta M, Johnson M, Jayaswal RK, Morrissey JA (2010) Copper stress induces a global stress response in *Staphylococcus aureus* and represses *sae* and *agr* expression and biofilm formation. Appl Environ Microbiol 76(1):150–160. https://doi.org/10.1128/AEM.02268-09

Bondarczuk K, Piotrowska-Seget Z (2013) Molecular basis of active copper resistance mechanisms in Gram-negative bacteria. Cell Biol Toxicol 29(6):397–405. https://doi.org/10.1007/s10565-013-9262-1

Buckley BR, Neary SP, Elsegood MRJ (2010) The first enantiomerically pure thiadiazol-3-one 1-oxide and thiatriazaindene 3-oxide systems chiral at the sulfur atom. Tetrahedron 21(16):1959–1962. https://doi.org/10.1016/j.tetasy.2010.07.025

Butler HM, Hurse A, Thursky E, Shulman A (1969) Bactericidal action of selected phenanthroline chelates and related compounds. Aust J Exp Biol Med Sci 47:541–552

Campos-Vallette ME, Clavijo RE, Mendizabal F, Zamudio W, Baraona R, Diaz G (1996) Infrared spectrum of the bis-

(1,10-phenanthroline) Cu(I) and Cu(II) perchlorate complexes. Vib Spectrosc 12:37–44

Capilato JN, Philippi SV, Reardon T, McConnell A, Oliver DC, Warren A, Adams JS, Wu C, Perez LJ (2017) Development of a novel series of non-natural triaryl agonists and antagonists of the *Pseudomonas aeruginosa* LasR quorum sensing receptor. Bioorg Med Chem 25(1):153–165. https://doi.org/10.1016/j.bmc.2016.10.021

Centers for Disease Control and Prevention (2013) Antibiotic resistance threats in the United States, 2013 (Report). https://www.cdc.gov/drugresistance/threat-report-2013/pdf/ar-threats-2013-508.pdf

Centers for Disease Control and Prevention (2014) Active bacterial core surveillance (ABCs) report emerging infections program network methicillin-resistant *Staphylococcus aureus*. www.cdc.gov/abcs/reports-findings/survreports/mrsa14.html

Cook SM, McArthur JD (2013) Developing *Galleria mellonella* as a model host for human pathogens. Virulence 4(5):350–353. https://doi.org/10.4161/viru.25240

Coyle B, McCann M, Kavanagh K (2004) Synthesis, X-ray crystal structure, anti-fungal and anti-cancer activity of $[Ag_2(NH_3)_2(salH)_2]$ ($salH_2$ = salicylic acid). J Inorg Biochem 98:1361–1368. https://doi.org/10.1016/j.jinorgbio.2004.04.016

DeLeo FR, Chambers HF (2009) Reemergence of antibiotic-resistant *Staphylococcus aureus* in the genomics era. J Clin Investig 119(9):2464–2474. https://doi.org/10.1172/JCI38226

Dinh H, Semenec L, Kumar SS, Short FL, Cain AK (2021) Microbiology's next top model: galleria in the molecular age. Pathog Dis 79(2):ftab006

Dwyer FP, Reid IK, Shulman A, Laycock GM, Dixson S (1969) Biological actions of 1,10-phenanthroline and 2,2'-bipyridine hydrochloride, quaternary salts, and metal chelates and related compounds. I. Bacteriostatic action on selected gram-positive, gram-negative, and acid-fast bacteria. Aust J Exp Biol Med Sci 47:203–218. https://doi.org/10.1038/icb.1969.21

German N, Doyscher D, Rensing C (2013) Bacterial killing in macrophages and amoeba: do they all use a brass dagger? Future Microbiol 8:1257–1264

Graf N, Lippard SJ (2012) Redox activation of metal-based prodrugs as a strategy for drug delivery. Adv Drug Deliv Rev 64(11):993–1004. https://doi.org/10.1016/j.addr.2012.01.007

Guo Z, Sadler PJ (1999) Metals in medcine [metals in medcine]. Angew Chem Int Ed 38:1512–1531

Haeili M, Moore C, Davis CJ, Cochran JB, Shah S, Shrestha TB, Zhang Y, Bossmann SH, Benjamin WH, Kutsch O, Wolschendorf F (2014) Copper complexation screen reveals compounds with potent antibiotic properties against methicillin-resistant *Staphylococcus aureus*. Antimicrob Agents Chemother 58(7):3727–3736. https://doi.org/10.1128/AAC.02316-13

Hambley TW (2007) Developing new metal-based therapeutics: challenges and opportunities. Dalton Trans 43:4929–4937. https://doi.org/10.1039/b706075k

Hannesschlaeger C, Horner A, Pohl P (2019) Intrinsic membrane permeability to small molecules. Chem Rev (washington, DC, US) 119(9):5922–5953. https://doi.org/10.1021/acs.chemrev.8b00560

Joondan N, Jhaumeer-Laulloo S, Caumul P (2014) A study of the antibacterial activity of L-phenylalanine and L-tyrosine esters in relation to their CMCs and their interactions with 1,2-dipalmitoyl-*sn*-glycero-3-phosphocholine DPPC as model membrane. Microbiol Res 169(9–10):675–685. https://doi.org/10.1016/j.micres.2014.02.010

Joseph J, Nagashri K, Ayisha Bibin Rani G (2013) Synthesis, characterization and antimicrobial activities of copper complexes derived from 4-aminoantipyrine derivatives. J Saudi Chem Soc 17(3):285–294. https://doi.org/10.1016/j.jscs.2011.04.007

Karlsson HL, Cronholm P, Hedberg Y, Tornberg M, De Battice L, Svedhem S, Wallinder IO (2013) Cell membrane damage and protein interaction induced by copper containing nanoparticles: importance of the metal release process. Toxicology 313(1):59–69. https://doi.org/10.1016/j.tox.2013.07.012

Kellett A, Fichtner I, Kavanagh K, Devereux M, Pyrrho AS, Romanos MTV, da Silva BA, Santos ALS, McCann M (2012) *In vitro* and *in vivo* studies into the biological activities of 1,10-phenanthroline, 1,10-phenanthroline-5,6-dione and its copper(ii) and silver(i) complexes. Toxicol Res 1(1):47–54. https://doi.org/10.1039/c2tx00010e

Krishnamoorthy G, Leus IV, Weeks JW, Wolloscheck D, Rybenkov VV, Zgurskaya HI (2017) Synergy between active efflux and outer membrane diffusion defines rules of antibiotic permeation into Gram-negative bacteria. Mbio 8(5):e01172-01117/01171-e01172-01117/01116. https://doi.org/10.1128/mBio.01172-17

Kumar SV, Scottwell SO, Waugh E, McAdam CJ, Hanton LR, Brooks HJ, Crowley JD (2016) Antimicrobial properties of tris(homoleptic) ruthenium(II) 2-pyridyl-1,2,3-triazole "Click" complexes against pathogenic bacteria, Including Methicillin-resistant *Staphylococcus aureus* (MRSA). Inorg Chem 55(19):9767–9777. https://doi.org/10.1021/acs.inorgchem.6b01574

Łęczkowska A, Vilar R (2012) Interaction of metal complexes with nucleic acids. Annu Rep Prog Chem Sect A Inorg Chem 108:330–349. https://doi.org/10.1039/c2ic90016e

Liu H, Yang W, Zhou W, Xu Y, Xie J, Li M (2013) Crystal structures and antimicrobial activities of copper(II) complexes of fluorine-containing thioureido ligands. Inorg Chim Acta 405:387–394. https://doi.org/10.1016/j.ica.2013.06.029

Luman CR, Castellano FN (2004) 1,2-Phenanthroline ligands. In: McCleverty JA, Meyer TJ (eds) Comprehensive coordination chemistry II, vol 1. Pergamon, Oxford, pp 25–39

Malachowa N, DeLeo FR (2010) Mobile genetic elements of *Staphylococcus aureus*. Cell Mol Life Sci 67(18):3057–3071. https://doi.org/10.1007/s00018-010-0389-4

Manning T, Mikula R, Lee H, Calvin A, Darrah J, Wylie G, Phillips D, Bythell BJ (2014) The copper (II) ion as a carrier for the antibiotic capreomycin against *Mycobacterium tuberculosis*. Bioorg Med Chem Lett 24(3):976–982. https://doi.org/10.1016/j.bmcl.2013.12.053

McCann M, McGinley J, Ni K, O'Connor M, Kavanagh K, McKee V, Colleran J, Devereux M, Gathergood N, Barron

N, Prisecaru A, Kellett A (2013) A new phenanthroline-oxazine ligand: synthesis, coordination chemistry and atypical DNA binding interaction. Chem Commun (cambridge, U.k.) 49(23):2341–2343. https://doi.org/10.1039/c3cc38710k

Memon S, Chandio AA, Memon AA, Panhwar QK, Nizamani SM, Bhatti AA, Brohi NA (2016) Synthesis, characterization, and exploration of antimicrobial activity of copper complex of diamide derivative of p-tert-butylcalix[4]arene. Polycycl Aromat Compd 37(5):362–374. https://doi.org/10.1080/10406638.2015.1125375

Mjos KD, Orvig C (2014) Metallodrugs in medicinal inorganic chemistry. Chem Rev (washington, DC, US) 114(8):4540–4563. https://doi.org/10.1021/cr400460s

Morell EA, Balkin DM (2010) Methicillin resistant *Staphylococcus Aureus* a pervasive pathogen highlights the need for new antimicrobial development. YJBM 83:223–233

Nunes P, Correia I, Marques F, Matos AP, dos Santos MMC, Azevedo CG, Capelo J-L, Santos HM, Gama S, Pinheiro T, Cavaco I, Pessoa JC (2020) Copper complexes with 1,10-phenanthroline derivatives: underlying factors affecting their cytotoxicity. Inorgan Chem 59(13):9116–9134. https://doi.org/10.1021/acs.inorgchem.0c00925

Payne DJ (2008) Microbiology. Desperately seeking new antibiotics. Science 321(5896):1644–1645. https://doi.org/10.1126/science.1164586

Piatek M, Sheehan G, Kavanagh K (2020) Utilising Galleria mellonella larvae for studying in vivo activity of conventional and novel antimicrobial agents. Pathog Dis 78(8):ftaa059

Pitchumani Violet Mary C, Shankar R, Vijayakumar S (2019) Theoretical insights into the metal chelating and antimicrobial properties of the chalcone based Schiff bases. Mol Simul 45(8):636–645. https://doi.org/10.1080/08927022.2019.1573370

Proteau-Gagné A, Véronique B, Kristina R, Dory YL, Gendron L (2010) Exploring the backbone of enkephalins to adjust their pharmacological profile for the δ-opioid receptor. ACS Chem Neurosci 1(11):757–769

Ronconi L, Sadler PJ (2007) Using coordination chemistry to design new medicines. Coord Chem Rev 251(13–14):1633–1648. https://doi.org/10.1016/j.ccr.2006.11.017

Roy S, Hagen KD, Maheswari PU, Lutz M, Spek AL, Reedijk J, van Wezel GP (2008) Phenanthroline derivatives with improved selectivity as DNA-targeting anticancer or antimicrobial drugs. ChemMedChem 3(9):1427–1434. https://doi.org/10.1002/cmdc.200800097

Salah I, Parkin IP, Allan E (2021) Copper as an antimicrobial agent: recent advances. RSC Adv 11(30):18179–18186. https://doi.org/10.1039/d1ra02149d

Sancak B, Yağcı S, Mirza HC, Hasçelik G (2013) Evaluation of vancomycin and daptomycin MIC trends for methicillin-resistant *Staphylococcus aureus* blood isolates over an 11 year period. J Antimicrob Chemother 68(11):2689–2691. https://doi.org/10.1093/jac/dkt247

Schito GC (2006) The importance of the development of antibiotoc resistance in *Staphylococcus aureus*. Clin Microbiol Infect 12:3–8

Shulman A, White DO (1973) Virostatic activity of 1,10-phenanthroline transition metal chelates A structure-activity analysis.pdf. Chem Biol Interact 6(6):407–403. https://doi.org/10.1016/0009-2797(73)90060-4

Viganor L, Galdino AC, Nunes AP, Santos KR, Branquinha MH, Devereux M, Kellett A, McCann M, Santos AL (2016) Anti-*Pseudomonas aeruginosa* activity of 1,10-phenanthroline-based drugs against both planktonic- and biofilm-growing cells. J Antimicrob Chemother 71(1):128–134. https://doi.org/10.1093/jac/dkv292

Viganor L, Howe O, McCarron P, McCann M, Devereux M (2017) The antibacterial activity of metal complexes containing 1,10- phenanthroline: potential as alternative therapeutics in the era of antibiotic resistance. Curr Top Med Chem (sharjah United Arab Emirates) 17(11):1280–1302. https://doi.org/10.2174/1568026616666161003143333

World Health Organization (2014) WHO. Antimicrobial Resistance Global Report on Surveillance. http://apps.who.int/iris/handle/10665/112642.

Yang Y, Zhou Y, Ge J, Wang Y, Chen X (2011) Synthesis, characterization and infrared emissivity property of optically active polyurethane derived from tyrosine. Polymer 52(17):3745–3751. https://doi.org/10.1016/j.polymer.2011.06.027

Zheng RH, Guo HC, Jiang HJ, Xu KH, Liu BB, Sun WL, Shen ZQ (2010) A new and convenient synthesis of phendiones oxidated by $KBrO_3/H_2SO_4$ at room temperature. Chin Chem Lett 21(11):1270–1272. https://doi.org/10.1016/j.cclet.2010.05.030